CARBON-DISC 1.0 - A coupled, process-based model of global in-stream carbon biogeochemistry

Wim J. van Hoek[1], Lauriane Vilmin[1], Arthur H.W. Beusen[1,2], José M. Mogollón[4], Xiaochen Liu[1], Joep J. Langeveld[1], Alexander F. Bouwman[1,2,3], Jack J. Middelburg[1]

5   1 Department of Earth Sciences, Utrecht University, P.O. Box 80021, 3508TA Utrecht, the Netherlands.
2 PBL Netherlands Environmental Assessment Agency, P.O. Box 30314, 2500GH the Hague, the Netherlands.
3 Laboratory of Marine Chemistry Theory and Technology, Ministry of Education, Ocean University of China, Qingdao 266100, PR China.
4 Department of Industrial Ecology, Leiden University, P.O. Box 9518, 2300RA Leiden, the Netherlands.

Abstract

Here, we present the implementation of the freshwater carbon (C) cycle in the Dynamic In-stream Chemistry module
15   (CARBON-DISC), which is part of the Integrated Model to Assess the Global Environment-Dynamic Global Nutrient Model (IMAGE-DGNM). A coupled hydrology-biogeochemistry approach with 0.5 by 0.5-degree resolution accounts for the spatial and temporal variability in dynamic conditions in the aquatic continuum using independent global databases. This process-based model resolves the concentrations, transformations and transfer fluxes of dissolved inorganic carbon (*DIC*), dissolved organic carbon (*DOC*) and terrestrial and autochthonous particulate organic carbon (*POC*) from headwaters to river mouth with a time step of 1 month for the period 1950-2000.

This is a major step forward in basin scale modelling of the C processing in freshwater systems, since simulated results can be validated at every location and point in time, and the model can be applied for retrodiction and to analyse future scenarios. Validation of the model with long-term measurement data shows a fair agreement, considering that this is a global model. To analyse the performance of the full production-respiration DISC module, two other schemes are presented, including an abiotic
25   system excluding any in-stream processing of *DOC* and allochthonous production, and an extended abiotic system including heterotrophic respiration, but excluding production. Furthermore, a sensitivity analysis shows that many parameters, such as temperature, solar radiation, organic sediment mineralization rate and C inputs, including particulate organic carbon from terrestrial vegetation and dissolved inorganic carbon from groundwater, strongly affect atmosphere-freshwater exchange of CO_2.

1. Introduction

Only recently, (Cole et al., 2007) identified rivers as significant components of the global carbon (C) cycle and recognized that
river systems function as globally important sources of CO_2. Since then, multiple studies have confirmed the significance of
freshwater systems in global carbon cycling, but there is substantial uncertainty on the magnitude of fluxes and the human
perturbation (Cole et al., 2007; Battin et al., 2009; Tranvik et al., 2009; Bastviken et al., 2011; Raymond et al., 2013; Regnier
et al., 2013; Borges et al., 2015; Holgerson and Raymond, 2016; Sawakuchi et al., 2017).

Carbon in freshwater originates from terrestrial (allochthonous) sources and from aquatic within system (autochthonous)
production (Prairie and Cole, 2009). Allochthonous C is delivered to surface water as dissolved or particulate organic C (plant
litter , leached material) or dissolved inorganic C (carbonates produced during weathering or soil respiration) (Cole et al.,
2007). After delivery to streams, rivers, lakes or reservoirs, organic C is metabolized to inorganic carbon, buried in sediment
or laterally transported towards oceans. The inorganic carbon delivered or generated within the system is transported
downstream or emitted to the atmosphere as CO_2 since aquatic systems are predominantly supersaturated in CO_2 relative to
the atmosphere (Kempe, 1984; Frankignoulle et al., 1998; Duarte and Prairie, 2005)

Many studies have been published on local C processing in headwaters, rivers, lakes, reservoirs and floodplains (Tranvik et
al., 2009; Crawford et al., 2013, 2016; Wallin et al., 2013; Hotchkiss et al., 2015; Wollheim et al., 2015; Holgerson and
Raymond, 2016). These local assessments have identified the key governing processes and their sensitivity to perturbations.
Global assessments of riverine carbon cycling, and in particular CO_2 partial pressure and global CO_2 effluxes have been very
important to quantify the role of rivers in the global C cycle. However, these budgeting approaches fail to describe the rapid
changes in the global C-cycle (Ciais et al., 2013)and are not appropriate for retrodictions (predictions of the past) or making
informed projections. Many existing river biogeochemistry models lack spatio-temporal input and hydrological constraints.
Moreover the models usually lump the various compartment of the aquatic continuum and regress modelled and observed C
export at the scale of whole river basins (Beusen et al., 2005; Mayorga et al., 2010; Kroeze et al., 2012) After upscaling, such
approaches yield a first order quantification of C fluxes to the coastal ocean. However, they contribute little to advance our
understanding of the C cycle in river basins. To describe the interactions between land-use changes, interventions in the
hydrology (dam construction, reservoirs, water extraction), and wastewater discharge, and their consequences for riverine C
cycling, we need a model that spatio-temporally resolves the biogeochemical processes coupled to hydrology.

In this paper we present the implementation of freshwater C cycling in the Dynamic In-stream Chemistry module (CARBON-
DISC), which is part of the Integrated Model to Assess the Global Environment (IMAGE (Stehfest et al., 2014)) Dynamic
Global Nutrient Model (IMAGE-DGNM (Vilmin et al., 2019)). This new model is specifically designed for global applications

65   and describes the spatial and temporal variability of carbon concentration and fluxes based on the river basin hydrology from
headwaters to mouth and carbon cycling processes. Here, we present the main features of the CARBON-DISC module, we
apply the module in the stream network of the Rhine basin and evaluate its characteristics with a sensitivity analysis.

2.   Model and data used

2.1 General aspects

70   The IMAGE-DGNM model framework integrates the PCR-GLOBWB dynamic global hydrology model (Sutanudjaja et al.,
2018) with the IMAGE model (Stehfest et al., 2014) that provides C, nitrogen (N) and phosphorus (P) delivery to inland waters
(streams, rivers, lakes, reservoirs, floodplains) for the period 1900-2000. The biogeochemistry within the streams, rivers, lakes,
reservoirs and floodplains is modelled using the DISC module, which is part of the IMAGE-DGNM framework (Vilmin et al.,
2019). The IMAGE-DGNM has a global coverage with a 0.5 degree spatial resolution and includes spatially resolved

75   biogeochemical input data ((Beusen et al., 2015); (Vilmin et al., 2019)). IMAGE-DGNM uses ancillary information of air
temperature from a CRU dataset (Mitchell and Jones, 2005) as a 1:1 proxy for the water temperature. Although the temporal
scale of the model framework is adjustable, here we focus on monthly-scale processes.

IMAGE provides land cover data to PCR-GLOBWB and wastewater, suspended particulate matter (SPM) and allochthonous

80   organic carbon loads to CARBON-DISC; PCR-GLOBWB provides water flows, depth and volume of water bodies for streams
of Strahler order > 5. The hydrology for smaller streams and rivers is parameterized in IMAGE-DGNM using the approach
proposed by (Wollheim et al., 2008), as described in Beusen et al., 2015 (Fig. 1). DGNM explicitly accounts for spatio-
temporal distribution of sources for the different forms of C. These include wastewater, erosion, weathering, vegetation in
riparian areas and floodplains (details are provided in Table 1). After delivery of C in the form of particulate organic carbon

85   (POC), dissolved organic carbon (DOC), dissolved inorganic carbon (DIC, the sum of CO_2, HCO_3^- and CO_3^{2-}) and alkalinity
(ALK) to streams and rivers (see Table 1), the DISC model calculates in-stream biogeochemistry and transport from Strahler
order 1 to the mainstream for each grid cell, and from upstream cells to the coastal ocean.
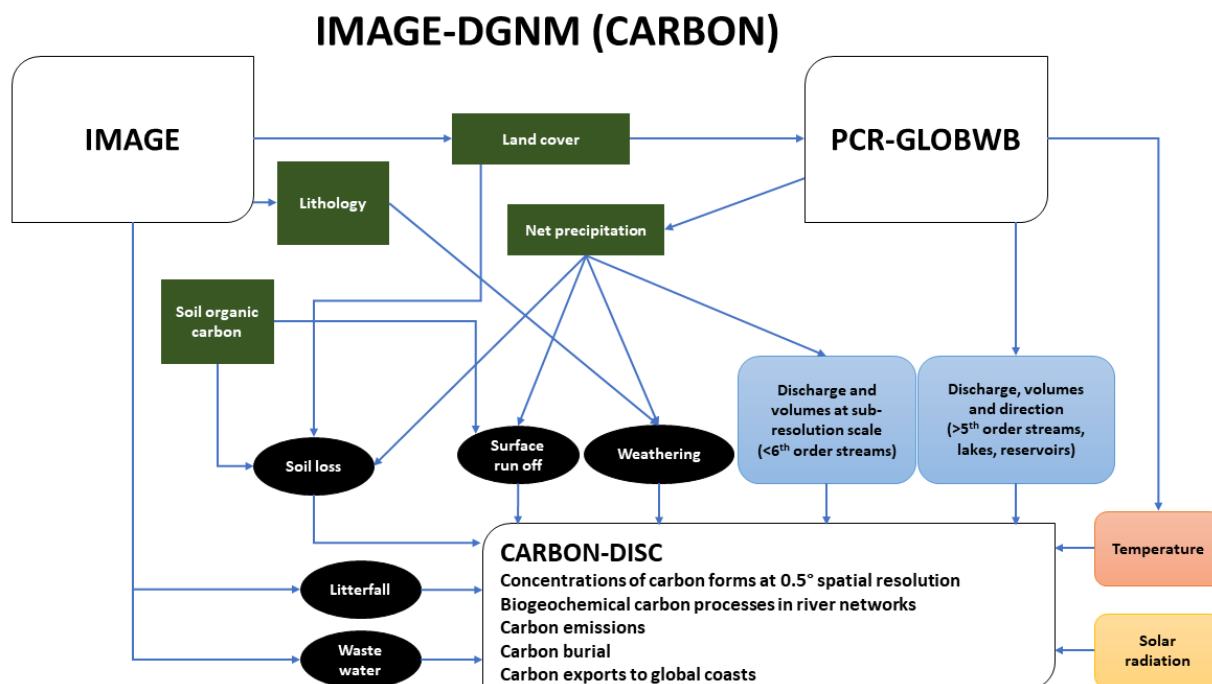
Figure 1: Scheme of the IMAGE-DGNM framework including CARBON-DISC for the in-stream biogeochemical carbon processes

90 IMAGE-DGNM explicitly resolves the mass and fluxes of suspended particulate matter (*SPM*) and sedimented particles. The pool of sedimented particles represents the mass of particles that have settled that can be resuspended as a result of exposure of the sediment surface to flowing waters. SPM is an important factor for light attenuation in the water column. (Kirk, 2011). *SPM* is delivered from land to surface waters through soil erosion and from litterfall by terrestrial vegetation and during transport, it is produced within the water column through primary production. *SPM* consists of non-reactive, particulate

95 inorganic matter (*PIM*) and reactive particles, particulate organic matter (*POM*). All suspended particulate species also exist in the sediment form. Calcium carbonate particles are not identified as a distinct unit.

The CARBON-DISC module describes the biogeochemical transformations of *DOC* and *POC* to *DIC*. These instream processes depend on hydrology, temperature and solar irradiance (Fig. 1). *POC* comprises hundreds of different compounds

100 varying from easily decomposable to recalcitrant (Middelburg, 1989; Bianchi, 2011). To account for the diversity in POC reactivity, we distinguish among allochthonous, terrestrial *POC* (*POC$_{terre}$* and *SEDOC$_{terre}$*) and aquatic, autochthonous *POC* (*POC$_{auto}$* and *SEDOC$_{auto}$*), because the mineralization of terrestrial organic matter with structural carbohydrates and lignins is slower than that of aquatic organic matter, rich in N and P (Middelburg, 2019). Physical dynamics of *POC* are governed by simplified deposition and resuspension equations.

105

Alkalinity (*ALK*) is generated by weathering of soils and rocks and delivered to streams. Although *ALK* is the sum of excess bases in solution in natural environments carbonate alkalinity ($HCO_3^- + 2\,CO_3^{2-}$) tends to make up most of the total alkalinity. In our model *ALK* is delivered to surface water and combined with model generated *DIC* to calculate pCO_2 and pH, but it is not modified by chemical reactions within the river. Consequently, CARBON-DISC ignores *ALK* production and consumption

110   by primary production, respiration, nitrification and calcium carbonate precipitation and dissolution within the stream network (Soetaert et al., 2007), since we assume that large scale alkalinity concentrations are governed by weathering of soils and rocks.

The performance of the model is validated by comparing simulation results of *DIC*, *ALK*, pCO_2, pH, *DOC* and *TOC* with literature data along the main stream (Fig. 2). Literature data were acquired from the GLORICH database (Hartmann et al.,

115   2014) (https://www.geo.uni-hamburg.de/en/geologie/forschung/geochemie/glorich.html). We compare monthly simulations and two weekly measurements of *DIC*, alkalinity, pCO_2, pH, *DOC* and TOC for the station in Lobith, located on the German-Dutch border. The model can simulate at any temporal resolution, but here we discuss the monthly aggregated results.
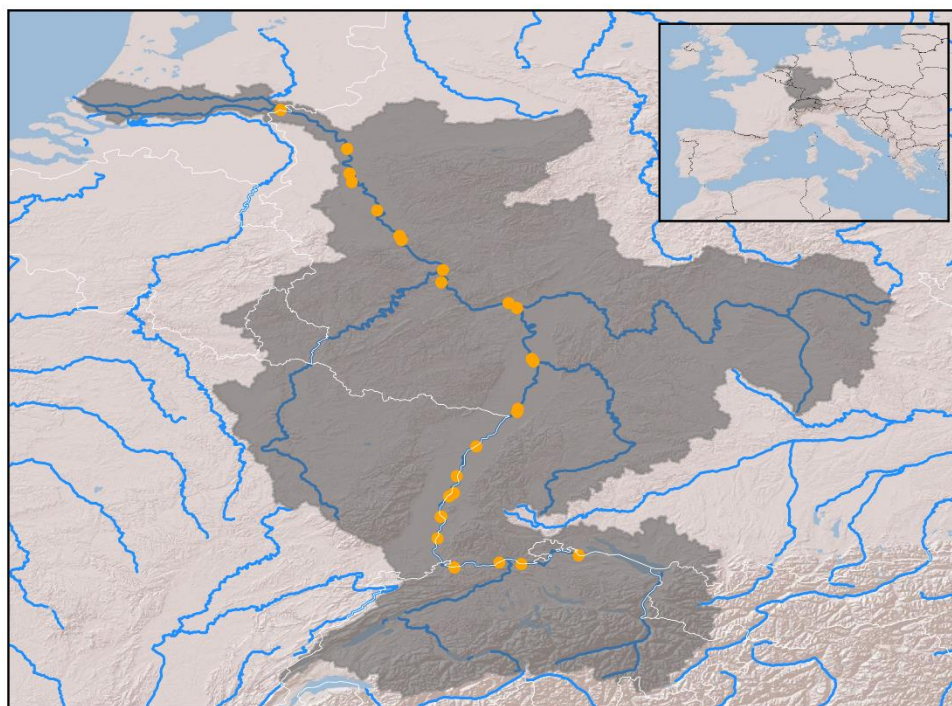
120

Figure 2: Map of Rhine basin with available in-stream carbon measurement locations for GLORICH (Hartmann et al., 2014)

2.2 Model description

125   CARBON-DISC provides the concentration of any C species i [Mmol/km^3] in each waterbody (i.e. a stream, lake, reservoir or floodplain) in each grid cell and for each time step (here 1 month) by calculating the total (*tot*) change in Mmol per time step of all C species i in each waterbody (i.e. a stream, lake, reservoir or floodplain) in each grid cell, as an effect of biogeochemical (*bgc*) interactions between C species and as a result of hydrological (*hyd*) transport from waterbody to waterbody, within a grid cell as well as from grid cell to grid cell, as follows:

130

$$\frac{dC_i}{dt}_{tot} = \begin{cases} \frac{dC_i}{dt}_{bgc} + \frac{dC_i}{dt}_{hyd} & \textit{if species is dissolved or suspended in water column} \\ \frac{dC_i}{dt}_{bgc} & \textit{if species is attached or sedimented onto bed surface} \end{cases} \qquad (1)$$

Hydrological advection of any dissolved or particulate C species i in the water column, being *DIC*, *DOC*, *POC* and *ALG*, is calculated as follows:

135   $$\frac{dC_i}{dt}_{hyd} = L_i - Q * [C_i] \qquad (2)$$

with L_i representing the upstream load [Mmol/yr] of species C i. Q represents the water discharge [km^3/yr] and [C_i] represents the concentration of carbon species i [Mmol/km^3], which we obtain from dividing the total amount of species i [Mmol] in the water body by the volume [km^3] of that water body (acquired from hydrological model data). From 1st to 5th Strahler orders, discharge and water volumes are calculated through the approach proposed by (Wollheim et al., 2008), as described in Vilmin

140   et al. (submitted). For 6th Strahler order and higher, discharge and water body dimensions as well as floodplain area and depth data are provided by PCR-GLOBWB (Sutanudjaja et al., 2018) at a 0.5° spatial resolution. Floodplains are only exchanging water with the 6th Strahler order and higher in the same grid cell, and we assume their flow velocity is 10% of the main stream velocity. Hydrological transport from low to higher Strahler orders, and from one grid cell to the next grid cell, is calculated as long as these species are in the surface water column. *POC*, when sedimented as *SEDOC* (see below in Eq. (18)) remains

145   where it is settled until it is resuspended. ALG_{benth} is not being transported downstream, as it is considered attached to the stream bed.

2.2.1.   DIC dynamics

External input of *DIC* in the DISC module is from weathering (Table 1) and there is in-stream production of *DIC* through

150   mineralization of organic carbon forms and respiring living biomass. *DIC* is consumed through primary production. Finally, *DIC* is added to or removed from the water body in the form of CO_2 as a result of atmospheric exchange:

$dDIC/dt = WEA_{DIC} + DOC\_MINERALIZATION + POC_{terre}\_MINERALIZATION + POC_{auto}\_MINERALIZATION + SEDOC_{terre}\_MINERALIZATION + SEDOC_{auto}\_MINERALIZATION + ALG\_RESPIRATION + ALG_{benth}\_RESPIRATION -$
155    $ALG\_PRIMARY\_PRODUCTION - ALG_{benth}\_PRIMARY\_PRODUCTION - DIC\_ATMOSPHERIC\_EXCHANGE$ *(3)*

Atmospheric exchange is calculated from the difference in CO_2 concentrations between the surface water and the atmosphere:

$DIC\_ATMOSPHERIC\_EXCHANGE = k_{air} * (CO_{2water} - CO_{2atmosphere})$ *(4)*

160

Where $CO_{2atmosphere}$ is the atmospheric concentration, fixed at 0.0136 mmol L^{-1} (equivalent of 400 ppmv). CO_{2water} is the dissolved CO_2 concentration that is calculated (together with pH) from [DIC] [mmol L^{-1}], [ALK] [meq L^{-1}] and temperature with the MOCSY2.0 scheme from (Orr and Epitalon, 2015). Here, alkalinity delivery to surface waters is the same as DIC delivery, from WEA_{DIC}. Alkalinity is transported downstream without biogeochemical modifications. k_{air} is the atmospheric
165   exchange coefficient [h^{-1}] calculated as follows:

$k_{air} = k_{600} / (600/Sc_T)^{-0.5}$ *(5a)*

where k_{600} is the normalized k_{air} at 20°C and Sc_T is the Schmidt number at temperature T [C°] (Wanninkhof, 2014), calculated
170   from:

$Sc_T = 1911.1 - 118.11T + 3.4527T^2 - 0.04132T^3$ *(6)*

where T is represented by air temperature (Mitchell and Jones, 2005). The atmospheric exchange coefficient k_{600} can be estimated from flow velocity (v [cm s^{-1}]) for small rivers or from windspeed ($\bar{u}_{10}$ [m s^{-1}]) for large rivers (Alin et al., 2011):

175

$k_{600} = \begin{cases} a_1 + b_1 \ \bar{u}_{10} & if \ stream \ width > 100 \ meters \\ a_2 + b_2 * v & if \ stream \ width < 100 \ meters \end{cases}$ *(7)*

Values for a_1, b_1, a_2 and b_2 are by default set to respectively 4.46, 7.11, 13.82 and 0.35 (Alin et al., 2011).

180   k_{air} above floodplains is strongly reduced with factor F_{u10_veg} (0.001) when (a fraction of) high vegetation (F_{high_veg}) covers the floodplain. Vegetation type data from IMAGE (Stehfest et al., 2014) was classified as either high or low vegetation. A spatial fraction of high vegetation (F_{high_veg}) per 30 minutes gridcell was obtained from 5-minutes resolution IMAGE output. Equation (5a) is modified for floodplains as follows:

185    $k_{air\_floodplains} = (k_{600} / (600/Sc_T)^{-0.5}) * F_{high\_veg} * F_{u10\_veg} + (k_{600} / (600/Sc_T)^{-0.5}) * (1-F_{high\_veg})$ *(5b)*

2.2.2. Organic carbon dynamics

Surface runoff and waste water deliver *DOC* (Table 1), which is mineralized during its transport downstream. In-stream *DOC* production occurs through excretion by pelagic and benthic algae. *DOC* is consumed by mineralization.

190 $dDOC/dt = SRO_{DOC} + WAS_{DOC} + ALG\_EXCRETION + ALG_{benth}\_EXCRETION - DOC\_MINERALIZATION$

(8)

POC_{terre} has a terrestrial origin and originates from litterfall and soil erosion (Table 1). There is resuspension through in-stream erosion and sedimentation. Finally, POC_{terre} can be consumed by mineralization:

195 $dPOC_{terre}/dt = LIT_{POC}+ SOI_{POC} + SEDOC_{terre}\_INSTREAM\_EROSION - POC_{terre}\_SEDIMENTATION - POC_{terre}\_MINERALIZATION$

(9)

POC_{auto} is the autochthonous particulate organic carbon produced in-stream, via the death of primary producers. Similar to POC_{terre}, within river produced POC can be resuspended (erosion), deposited, or mineralized.

200

$dPOC_{auto}/dt = ALG\_C\_MORTALITY + ALG\_C\_benth\_MORTALITY+ SEDOC_{auto}\_INSTREAM\_EROSION – POC_{auto}\_SEDIMENTATION – POC_{auto}\_MINERALIZATION$

(10)

Particulate organic matter that has settled from the water column ($SEDOC_{terre}$ and $SEDOC_{auto}$) can either be resuspended to the

205 water column, transformed into *DIC* via mineralization or become buried.

The relevant equations are:

$dSEDOC_{terre}/dt = POC_{terre}\_SEDIMENTATION – SEDOC_{terre}\_INSTREAM\_EROSION – SEDOC_{terre}\_ MINERALIZATION – SEDOC_{terre}\_BURIAL$

(11)

210 $dSEDOC_{auto}/dt = POC_{auto}\_SEDIMENTATION – SEDOC_{auto}\_INSTREAM\_EROSION – SEDOC_{auto}\_ MINERALIZATION – SEDOC_{auto}\_BURIAL$

(12)

The erosion of the individual sedimented C species is a fraction of the total erosion Φ_{ero_tot} [ton/yr]. Φ_{ero_tot} is calculated from the total mass of sediment in the water body (SED_{tot} [ton]), bedarea (A [km^2]), flow velocity (v [km/yr]), slope (S [km*km^{-1}]),

215 a fixed erosion coefficient k_{ero} [ton/km^2] of $2*10^4$ and a half-saturation constant k_{sed} [km] of $1*10^{-6}$:

$\Phi_{ero\_tot} = k_{ero} * (SED_{tot}/A) / (k_{sed} + SED_{tot}/A) * S * v * A$

(13)

with:

220

$$SED_{tot} = SEDIM + SEDOM_{terre} + SEDOM_{auto} \qquad (14)$$

SEDIM represents the mass [ton] of sedimented inorganic matter and $SEDOM_{terre}$ and $SEDOM_{auto}$ represent the masses [ton] of organic matter in the sediment of terrestrial and in-stream origin, respectively. Their masses are calculated from $SEDOC_{terre}$

225 and $SEDOC_{auto}$ as:

$$SEDOM_{terre} = SEDOC_{terre} / f_{C\_SEDOCterre} * MM_C \qquad (15)$$
$$SEDOM_{auto} = SEDOC_{auto} / f_{C\_SEDOCauto} * MM_C \qquad (16)$$

230 with $f_{C\_SEDOCterre}$ and $f_{C\_SEDOCauto}$ the mass fractions of C in $SEDOM_{terre}$ and $SEDOM_{auto}$ respectively, assumed to be 0.5. MM_C is the molar mass of C (12 g/mol).

To calculate erosion of individual particulate species we use:

$$\Phi_{ero\_POCterre} = (SEDOC_{terre} / SED_{tot}) * \Phi_{ero\_tot} \qquad (17a)$$
235 $$\Phi_{ero\_POCauto} = (SEDOC_{auto} / SED_{tot}) * \Phi_{ero\_tot} \qquad (17b)$$

Sedimentation of *POC* (*terre* and *auto*) is calculated with:

$$POC_{terre}\_SEDIMENTATION = vsed_{POCterre} / D * POC_{terre} \qquad (18a)$$
$$POC_{auto}\_SEDIMENTATION = vsed_{POCauto} / D * POC_{auto} \qquad (18b)$$

240

where $vsed_{POC}$ is the sediment deposition velocity which is assumed to be 4.38 [km yr^{-1}] or 0.5 m h^{-1} (Vilmin et al., 2019) for both the terrestrial and autochthonous POC. *D* is the stream depth [km].

The temperature-dependent mineralization rates for *DOC, POC (terre* and *auto)* and *SEDOC (terre* and *auto)* are formulated

245 as follows:

$$DOC\_MINERALIZATION = f_{min}(T) * k_{DOCmin} * DOC \qquad (19)$$
$$POC_{terre}\_MINERALIZATION = f_{min}(T) * k_{POCterre\_min} * POC_{terre} \qquad (20a)$$
$$POC_{auto}\_MINERALIZATION = f_{min}(T) * k_{POCauto\_min} * POC_{auto} \qquad (20b)$$
$$SEDOC_{terre}\_MINERALIZATION = f_{min}(T) * k_{SEDOCterre\_min} * SEDOC_{terre} \qquad (21a)$$
250 $$SEDOC_{auto}\_MINERALIZATION = f_{min}(T) * k_{SEDOCauto\_min} * SEDOC_{auto} \qquad (21b)$$

The temperature dependency is described with a standard Q10 function:

$$f_{min}(T) = \exp\left(\frac{T-T_{ref}}{10}\right)\ln(Q10) \tag{22}$$

with T_{ref} as 15° Celsius and Q10 set to 2 for all non-living organic species (Soetaert and Herman, 2008).

255

Burial is calculated with:

$$SEDOC_{terre}\_BURIAL = k_{burial} * SEDOC_{terre} \tag{23a}$$

$$SEDOC_{auto}\_BURIAL = k_{burial} * SEDOC_{auto} \tag{23b}$$

Burial only occurs when the SED_{tot} per bed area is more than 50 kg/m^2.

260

2.2.3. Primary producers

ALG and *ALG$_{benth}$* represent carbon in suspended and stream-bed attached primary producers, respectively. Primary producer biomass increases through fixation of *DIC* and decreases via respiration (to *DIC*), mortality (to *POC$_{auto}$*) or excretion (to *DOC*):

265 $$dALG/dt = ALG\_PRIMARY\_PRODUCTION - ALG\_RESPIRATION - ALG\_MORTALITY - ALG\_EXCRETION \tag{24}$$

$$dALG_{benth}/dt = ALG_{benth}\_PRIMARY\_PRODUCTION - ALG_{benth}\_RESPIRATION - ALG_{benth}\_MORTALITY - ALG_{benth}\_EXCRETION \tag{25}$$

Primary production depends on the biomass of the producers, their maximal growth rates, temperature, and light and *DIC*
270 availability. Similarly, respiration and excretion are modelled as a fraction of primary producer biomass and depend on temperature (standard Q10 functions, see Eq. (22)).

$$ALG\_PRIMARY\_PRODUCTION = f_{ALG\_pp}(T) * ALG_{I\_lim} * ALG_{DIC\_lim} * k_{ALG\_pp} * ALG \tag{26}$$

$$ALG_{benth}\_PRIMARY\_PRODUCTION = f_{ALGbenth\_pp}(T) * ALG_{benth\_I\_lim} * ALG_{benth\_DIC\_lim} * k_{ALGbenth\_pp} * ALG_{benth} \tag{27}$$

275 $$ALG\_RESPIRATION = f_{ALG\_resp}(T) * k_{ALG\_resp} * ALG\_C \tag{28}$$

$$ALG_{benth}\_RESPIRATION = f_{ALGbenth\_resp}(T) * k_{ALGbenth\_resp} * ALG_{benth} \tag{29}$$

$$ALG\_EXCRETION = f_{ALG\_excr}(T) * k_{ALG\_excr} * ALG \tag{30}$$

$$ALG_{benth}\_EXCRETION = f_{ALGbenth\_excr}(T) * k_{ALGbenth\_excr} * ALG_{benth} \tag{31}$$

280 Mortality of *ALG* and *ALG$_{benth}$* is attributed to viral lysis and modelled with a parasitic lysis factor (*vf*) of 20 when a threshold concentration of *ALG* and *ALG$_{benth}$* of 19 µmol C L^{-1} ($\approx$65 µg L^{-1} Chl a (Garnier et al., 2000)) is exceeded.

$$ALG\_MORTALITY = (f_{ALG\_mort}(T) * k_{ALG\_mort}) + (f_{ALG\_mort}(T) * k_{ALG\_mort}) * (1+vf) * ALG \tag{32}$$

$$ALG_{benth}\_MORTALITY = (f_{ALGbenth\_mort}(T) * k_{ALGbenth\_mort}) + (f_{ALGbenth\_mort}(T) * k_{ALGbenth\_mort}) * (1+vf) * ALG_{benth} \tag{33}$$

285

Primary production of *ALG* and *ALG$_{benth}$* includes a DIC limitation (*DIC_lim*) term that is calculated with a Michaelis-Menten function as follows:

$$ALG_{DIC\_lim} = \frac{[DIC]}{k_{DIC}+[DIC]} \tag{34}$$

Light limitation for both pelagic and benthic primary producers is calculated using a spatial and temporal distribution of solar

290 radiation reaching the surface of the water body and a water turbidity (η_{tot}) that affects light penetration through the water column. Cloudless average solar radiation per month of the year (MOY) per latitude (lat) is calculated by dividing the month-integral solar radiation by the number of hours per month (HPM) as below:

$$I_0(MOY,lat) = \frac{\int_0^t I_0(t,lat)dt}{HPM} \tag{35}$$

where I_0, the solar radiation above the water surface, is integrated over time. Light limitation (*I_lim*) is calculated separately

295 for benthic primary producers (*ALG$_{benth}$*) and for pelagic primary producers (*ALG*). For the pelagic primary producers, limitation by light is integrated over the water column from water surface to the water body bottom at depth *z*, whereas for the benthic primary producers, production only takes place at the bottom, at depth *z*, of the water body. This is formulated as follows:

$$I\_lim(MOY,lat) = \begin{cases} \dfrac{I_z}{\left(I_z + k_{I_{ALG_{C_{benth}}}}\right)} & for\ ALG_{benth} \\ \dfrac{\int_0^z I_0(MOY,lat)}{\left(\int_0^z I_0(MOY,lat) + k_{I_{ALG_C}}\right)} & for\ ALG \end{cases} \tag{36}$$

300

with the light intensity I_z at depth *z* modelled using the Lambert-Beer equation:

$$I_z = I_0(MOY,lat) * e^{-\eta_{tot}*z} \tag{37}$$

The turbidity η_{tot} is calculated by adding all contributions to light attenuation (Scheffer, 2004). The turbidity η_{tot}, with

305 $\eta_{water}=0.8$ and $\eta_{PIM}=0.03$, is calculated according to:

$$\eta_{tot} = \eta_{water} + \eta_{POCterre} * [POC_{terre}] + \eta_{POCauto} * [POC_{auto}] + \eta_{ALG} * [ALG] + \eta_{DOC} * [DOC] + \eta_{PIM} * [PIM] \tag{38}$$

I_0, represents the solar radiation above the water surface and is calculated according to:

310 $$I_0(t, lat) = \theta_s(t, lat) * tt * I_{solar\_constant} \tag{39}$$

with $\theta_s(t, lat)$ as the solar zenith angle. Zenith is the hemispheric point above the location of reference. Transmissivity (tt) is fixed at 0.8 [-] and the solar constant ($I_{solar\_constant}$) fixed at 1367 W m^{-2}.

315 The solar zenith angle is calculated from:

$$\theta_s(t, \text{lat}) = \arccos((\sin(\text{lat}) * \sin(\delta(t)) + \cos(\text{lat}) * \cos(\delta(t)) * \cos(h(t, \text{lat})))) \qquad (40)$$

with δ as the solar declination angle. The solar declination angle is the angle the sun makes with the Earth's equatorial plane. h is the hour angle, which is the radian angle the earth has turned around, since the previous midnight at the location of

320 reference at time t.

The solar declination is calculated as follows:

$$\delta(t) = 23.45 * \pi/180 * \sin(2\pi*(284+\text{DOY}(t))/362.5) \qquad (41)$$
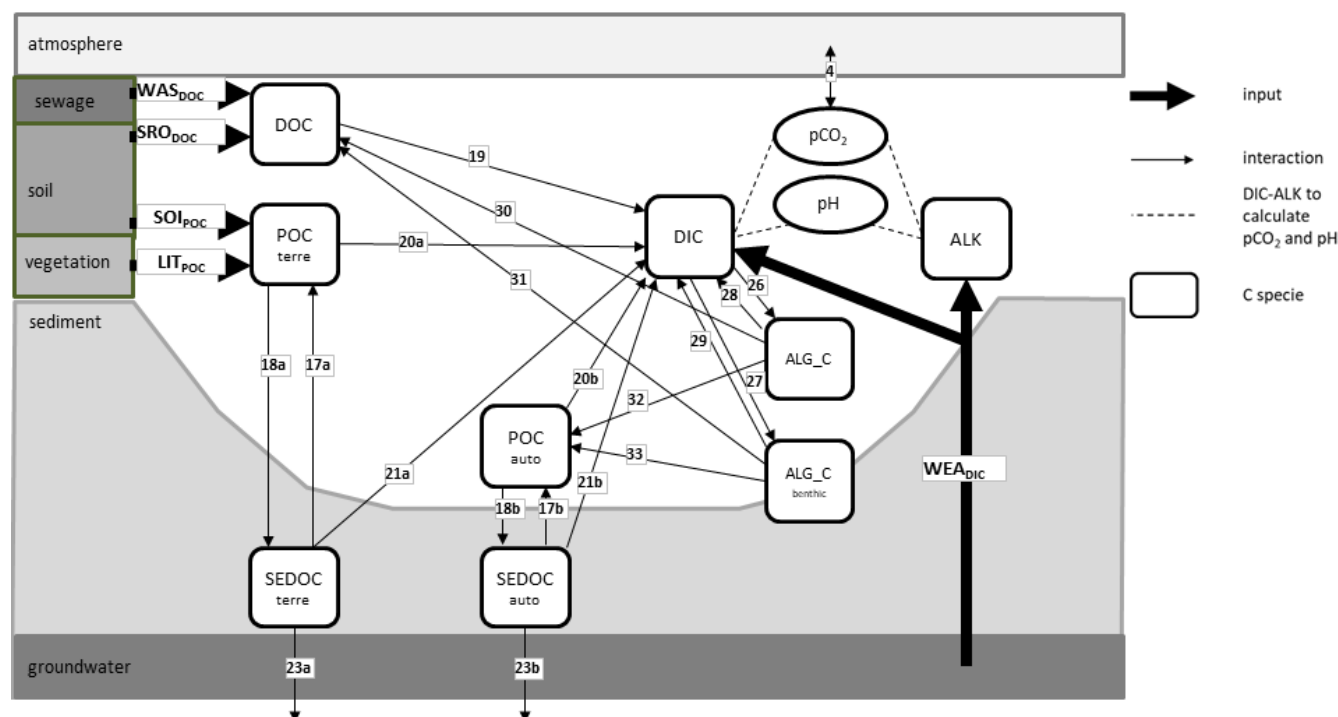
325

Figure 3: C forms, C sources and biogeochemical interactions in all simulated waterbodies. For clarity purposes, these schemes do not show the lateral influx and export. The numbers correspond to the equations in the text.

2.3 Model and sensitivity analysis

330 To analyse the performance of the full biology DISC model (Fig. 3), we present two other simplified in-stream C processing schemes:

1) the abiotic reference, with only POC, DOC and DIC external sources, transport, and atmospheric CO_2 exchange, and excluding any in-stream processing of DOC and production, mortality and mineralization of autochthonous C.

335   2) the respiration-only run, i.e. an extended abiotic system including respiration, but excluding autochthonous production. The numbers of the equations correspond with the numbers in Fig. 3.

Model parameter values and inputs are presented in Tables 2 and 3. The schemes of the abiotic and the respiration system respectively can be found in the supplementary material file.

340

Also, to further evaluate the model performance, we calculated the sensitivity of the modelled 5-year average (1995-2000) CO_2 emissions, total carbon export and POC retention to the variation of 45 parameters, 8 environmental constraints and 8 carbon sources using Latin Hypercube Sampling (Saltelli, 2000). The method allows to quantify sensitivity of model outcomes to varying parameters values with a relatively limited number of runs. We ran the model 750 times with a uniformly

345   randomized combined set of all model parameters, external constraints and external inputs. In each run, each model parameter, constraint and input is randomly multiplied with a factor between 0.95 and 1.05 and combined into a setting for one run. For temperature, the randomization is applied between -1K and +1K of the default temperature. Values used for the parameters, constraints and inputs are presented in the supplementary material.

350   The contribution of each parameter (X_i) to model outcome Y is assessed with linear regression (Saltelli, 2000: in Beusen et al 2015):

$$Y = \beta_0 + \beta_1 X_1 + \beta_2 X_2 \ldots + \beta_n X_n + e \tag{42}$$

355   with β_i as the ordinary regression coefficient of parameter i and e the error of the approximation of Y. The linear regression model can be evaluated for parameter contribution analysis if the coefficient of determination (R^2) is close to 1, i.e. when there is no variation of Y that is not explained with the linear regression model. A standardized regression coefficient (SRC_i) is used to scale β_i to the relative contribution of variation of Y, by using the standard deviations of X_i and Y as follows:

360    $$SRC_i = \beta_i \frac{\sigma_{X_i}}{\sigma_Y} \tag{43}$$

SRC_i is independent of units and scale of parameters. The SRC_i has a value between -1 and 1. A positive SRC_i value indicates that an increased parameter value leads to an increased output Y. A negative SRC_i indicates a decreased output Y with an increased parameter value. SRC_i^2 / R^2 yields the contribution of each parameter X_i to model outcome Y.

3. Results

The DISC module has been developed for global application, but, in this paper, we apply the model to the stream network of the Rhine basin without parameter tuning. The river Rhine drains an important part of Western Europe with an area of 185620 km^2 and a length of 1250 km (van der Weijden and Middelburg, 1989). The annual average discharge is 2300 m^3/s. The hydrology of the Rhine is strongly impacted by dams. Furthermore, with a population of 58 million inhabitants, it drains strongly urbanized landscapes with intensive agricultural systems (Uehlinger et al., 2009). The river Rhine has been monitored over decades for a range of monitoring stations. We present the IMAGE-DGNM results for the period 1950-2000, with estimates of the carbon delivery, retention, biogeochemical transformation, export and emission to the atmosphere for the entire watershed.

3.1 Carbon flows in the Rhine basin

Irrespective of the complexity of the biological processing, the river Rhine represents a source of CO_2 to the atmosphere (Fig. 4). In the abiotic scheme (Fig. 4(a)), CO_2 emissions are very low (0.02 Tg C/yr), while emissions in the respiration-only scheme (Fig. 4(b)) and in the biological scheme (Fig. 4(c)) are 118 (2.36 Tg C/yr or 41% of total C inputs) and 93 times higher (1.85 Tg C/yr or 32% of total C inputs), respectively. This indicates that outgassing of delivered CO_2 from external sources is very limited compared to within system generation of CO_2 by respiration. Furthermore, the difference between the respiration-only and biology scheme with respect to the basin CO_2 emissions suggests that in-stream biological processing is an important aspect in regulating CO_2 emissions from the aquatic continuum. The export of *DIC* is only 7% and 6% higher in the respiration-only (1.35 Tg/yr or +0.9 Tg/yr) and biology scheme (1.33 Tg/yr or +0.7 Tg/yr) respectively, than in the abiotic scheme (1.26 Tg /yr), while in-stream production of *DIC* is 2.42 and 3.71 Tg C/yr for respectively the respiration and the biology scheme versus 0 Tg C/yr in the abiotic scheme (Fig. 5). Nearly all CO_2 that is produced and consumed through in-stream biogeochemistry is emitted to the atmosphere in both the respiration-only and the biology schemes.
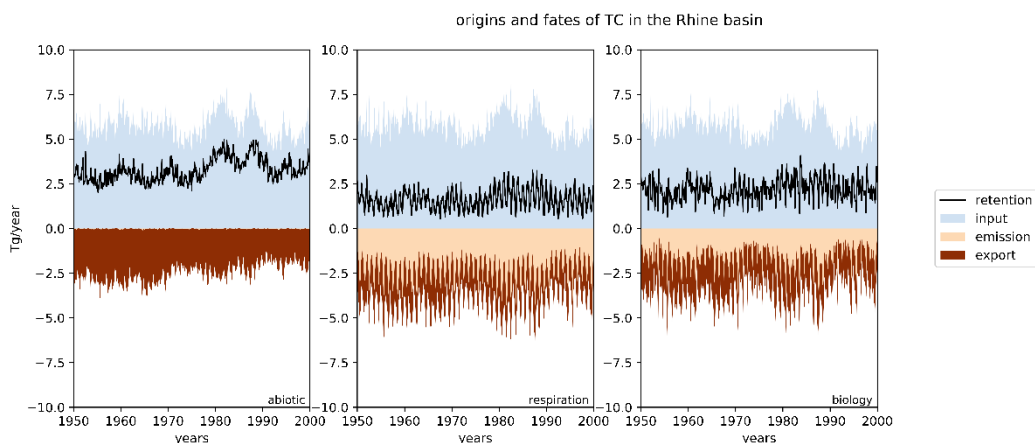
Figure 4: Time series of total basin aggregated carbon budget for the abiotic (a), respiration (b) and biology (c) schemes

390

In the abiotic scheme, about 3.25 Tg C/yr (57%) is retained in the Rhine basin, while total C retention in the respiration-only and biological schemes is 1.66 Tg/yr (29% of total C input) and 2.07 Tg/yr (36% of total C input), respectively (Fig. 5). The difference in C retention between the respiration-only and the biology scheme implies that in-stream biological processing is a necessary element to consider when quantifying basin retention of carbon. Total carbon delivery is 5.8 Tg/yr in all schemes,

395 but total C export to the ocean in the abiotic scheme is 2.48 Tg/yr (43% of total C input), and 1.78 Tg/yr (31% of total C input) and 1.88 Tg/yr (32% of total C input) in the respiration and biology schemes, respectively.

DIC, *DOC* and *POC_{terre}* average inputs into freshwaters of the Rhine basin are 1.3, 0.96 and 3.51 Tg/yr, or 23, 17 and 60 % of the total C input, respectively (Fig. 5). In the abiotic scheme, *DOC* delivery is fully balanced by export. In the respiration-only

400 and biology schemes, *DOC* delivered to the aquatic system is partly exported (0.27 Tg/yr, 28% *DOC* of input, and 0.34 Tg/yr, 35% *DOC* of input, respectively). In-stream removal of *DOC* through mineralization is 0.69 Tg/yr (72% of *DOC* input) and 0.82 Tg/yr (85% of input). In the biology scheme, an additional 0.2 Tg/yr (21% of *DOC* input) of *DOC* is produced in-stream by algal excretion. Export of *DOC* for the abiotic, respiration-only and biology schemes is 0.96, 0.27 and 0.34 Tg/yr, respectively.

405

About 0.26 Tg/yr (7% of *POC* input) of the *POC* delivered to the freshwater system (3.51 Tg/yr) is exported in the abiotic scheme. In the respiration-only and biology scheme, export of *POC* is 0.16 Tg/yr (5% of *POC* input) and 0.2 Tg/yr (6% of *POC* input), respectively. For the biology scheme, *POC* includes *POC_{terre}* and *POC_{auto}*. *POC* removal is 3.25 Tg/yr (93% of total *POC* input) in the abiotic scheme, and 3.35 Tg/yr (95% of *POC* input) and 4.69 Tg/yr (134% of *POC* input) in the

410 respiration-only and full biology respectively. In-stream production of POC (1.38 Tg/yr) in the biology scheme through primary production results in a higher *POC* removal rate than *POC* input.
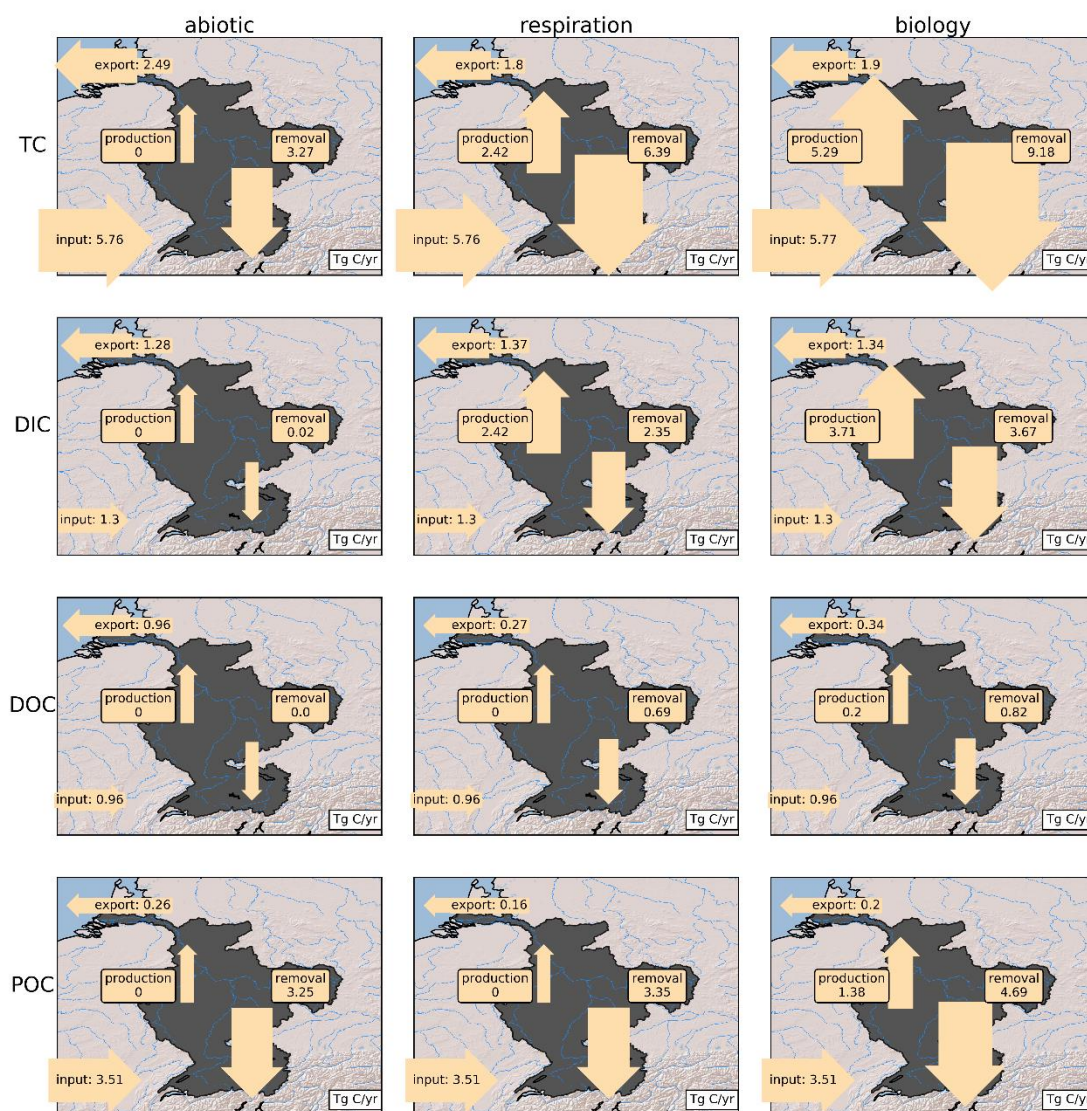
Figure 5: 50 year (1950-2000) average modelled input, production, removal and export fluxes of the Rhine basin of total carbon (TC) and C species for the three biogeochemical schemes (i.e., abiotic, respiration and biology).

415

3.2 Validation

Basin average *DIC* concentrations are higher by a few mg/L in the respiration and biology scheme compared to the abiotic one, as an effect of in-stream production of *DIC* by respiration. Alkalinity concentrations are identical among the different schemes, since the imported bicarbonate is not biogeochemically active during its transport through the aquatic continuum.

420 Simulated *DIC* and alkalinity concentrations in the biology scheme are on average respectively 46% and 43% lower than

observations (Fig. 6(b) and 6(e)) and are also weakly correlated with measurements (bicarbonate $r^2= 0.01$; *DIC* abiotic: $r^2=0.05$; *DIC* respiration: $r^2=0.07$; *DIC* biology: $r^2=0.07$). The weak correlation is likely related to the parameterization of the riverine alkalinity flux (Jansen, 2010), which depends on the coarse spatial distribution of the lithology and riverine discharge. The lithological data (Dürr et al., 2005) used here show only the dominant lithological class in 0.5 by 0.5-degree resolution.

425 Furthermore, runoff calculated by PCR-GLOBWB is prone to uncertainty and may be systematically underestimated in source areas of alkalinity.

Simulated average values of pCO_2 in the respiration-only and biology schemes are high (Fig. 6(d): 1399 and 1183 ppm, respectively), but much lower than average values of 5261 ppm from the GLORICH database. This underestimation can be

430 partly attributed to underestimated *DIC* and alkalinity, but values based on indirect measurements may also be strongly biased (Abril et al., 2015). Moreover, direct pCO_2 measurement in the Rhine using an equilibrator device vary from 545 to 1990 ppm (Frankignoulle et al., 1998).

The average simulated abiotic (8.0), respiration-only (7.6) and biology (7.7) pH values (Fig. 6(a))] show a fairly good

435 agreement with average measurements (pH=7.6), with a low r^2 for the abiotic run ($r^2=0.04$), and higher ones for the respiration and biology schemes ($r^2=0.31$ and $r^2=0.29$ respectively). The simulated *DOC* (Fig. 6(f)) and TOC (Fig. 6(c)) concentrations compare well with measurements (*DOC* [abiotic: $r^2= 0.73$; respiration: $r^2=0.79$; biology: $r^2=0.81$]; TOC [abiotic: $r^2=0.88$; respiration: $r^2=0.95$; biology: $r^2=0.95$]), with the abiotic scheme leading to overestimated TOC and *DOC* compared to measurements (DOC_measurements: 2.8 mg/L. and DOC_abiotic: 7.4 mg/L [> 159%]; TOC_measurements: 3.6 mg/L and

440 TOC_abiotic: 14.3 mg/L [>297%]) and the respiration and biology scheme underestimating *DOC* and TOC (DOC_respiration: 3.6 mg/L [>29%] and DOC_biology: 3.7 mg/L [>31%]; TOC_respiration: 8.8 mg/L [>144%] and TOC_biology: 9.0 mg/L [<150%]).
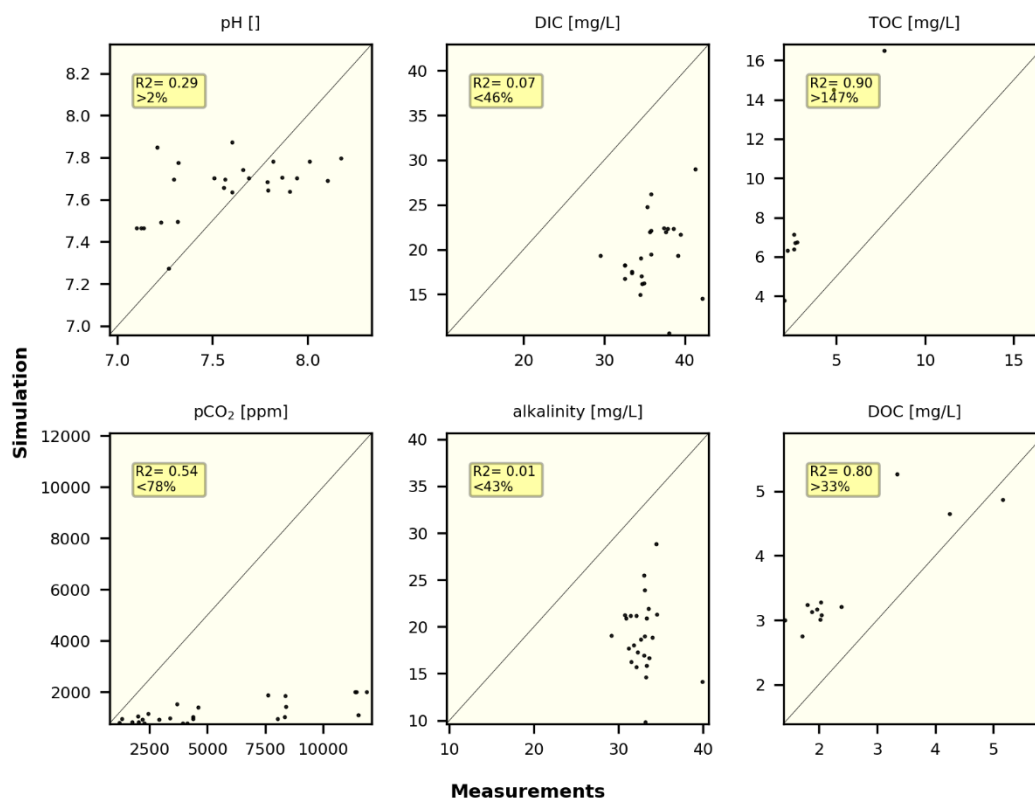
Figure 6: Comparison between average measurements (x-axis) and average simulations (biology scheme) for all available stations in the Rhine basin. Measurements are from the GLORICH database (Hartmann et al., 2014)

Figure 7 shows a 50-year simulation (for the abiotic, respiration-only and biology schemes) and measurement time series for station Bimmen/Lobith at the German/Dutch border. Differences among simulation results of the different schemes are most apparent for the organic forms of carbon (*DOC* and TOC). In the abiotic simulations all delivered organic C remains organic and concentrations are high, whereas in the other two schemes, organic forms are mineralized to *DIC*, resulting in lower concentrations of organic forms and elevated pCO_2. Time series of all other available measurement locations are found in the supplementary material section E (validation data).
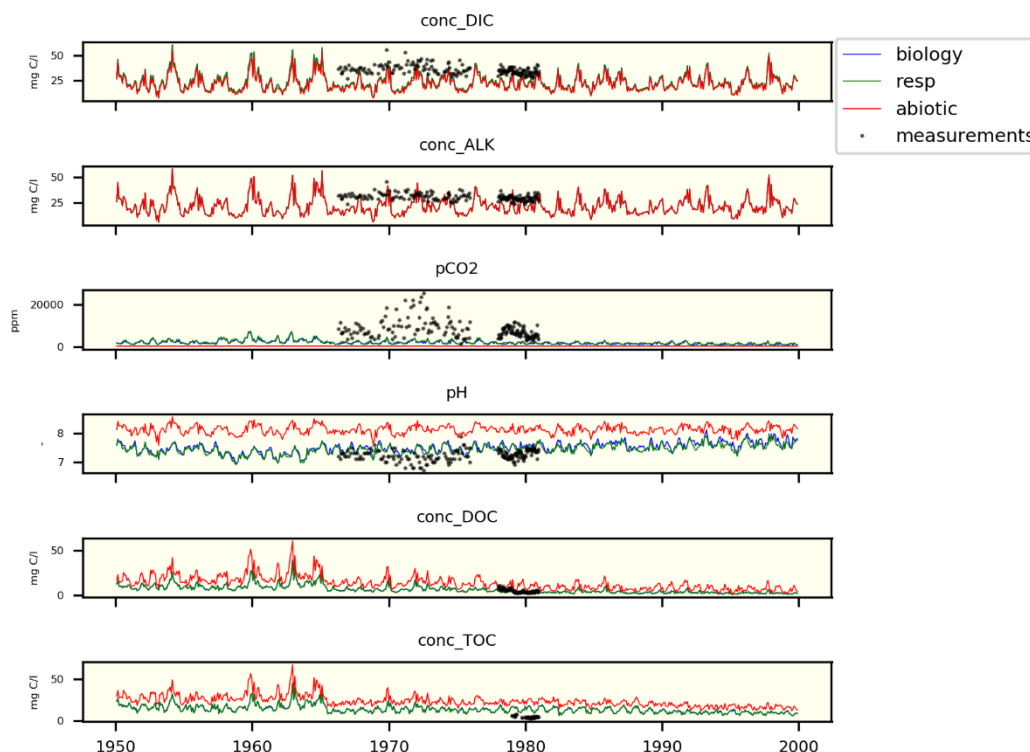
Figure 7: Timeseries of measurements and simulations at Bimmen/Lobith, Germany. Measurements are from the GLORICH database (Hartmann et al., 2014)

3.3 Sensitivity analysis

The influence of a range of parameters on simulated CO_2 emissions, C export and C retention was investigated, but we discuss only those parameters that have an influence of more than 20% on the variation of simulated CO_2 emissions, C export or C retention. Table 4 shows the most important outcomes of the sensitivity analysis. The entire table, containing all assessed parameters and SRC results is available in the supplementary materials section F (sensitivity analysis).

Simulated total basin CO_2 emissions are strongly influenced by many model parameters. Total basin CO_2 exchange is positively influenced by litter input in floodplains (SRC = 0.45), *DIC* fluxes from groundwater (SRC = 0.43), the organic sediment mineralization rate (SRC = 0.28) and temperature (SRC = 0.27). The CO_2 exchange is negatively influenced by alkalinity flux from groundwater (SRC= -0.42), global radiation (SRC = -0.24) and burial rate (SRC = -0.22). Except for the floodplains, CO_2 emissions are largely governed by *DIC* and *ALK* inputs that originate from groundwater. CO_2 emissions from floodplains are predominantly sensitive to temperature, global radiation, organic sediment mineralization rate, burial rate, minimum sediment thickness and most dominantly by input of POC from terrestrial vegetation.

The sensitivity analysis shows that variability of total C export (of which *DIC* is the dominant C species) is almost entirely governed by variability of alkalinity delivery from groundwater, i.e. weathering (SRC = 0.9). Almost all other carbon eventually escapes to the atmosphere.

475

The most important controlling factor of the modelled retention of POC_{terre} is the mineralization rate of $SEDOC_{terre}$, $k_{SEDOCterre\_min}$, which is governed by temperature. More mineralization enables more C to escape from the system as *DIC*. As expected, the burial rate also strongly affects *POC* retention. Furthermore, an increased input of POC_{terre} from litterfall leads to an increased total retention fraction.

480

Many regression models use discharge as a driver of river C export at the river basin scale (Beusen et al., 2005; Mayorga et al., 2010; Kroeze et al., 2012; Strokal et al., 2016), our sensitivity analysis suggests that discharge has a minor direct influence on the C biogeochemistry, retention and emissions and only total C export was strongly influenced by discharge (SRC=0.34). This concerns the river Rhine, and analysis of the results for other rivers is needed to assess if this is a general or local feature.

485   **4.   Conclusions**

The DISC module of IMAGE-DGNM is a major step forward in basin scale modelling of river systems. For the first time, we are able to make an integral and systemic simulation of biogeochemical C processing on the river basin scale in fair agreement with observations. Results show that process-based modelling is essential to assess the fate of C in river basins. Biogeochemical production and consumption of C within its lifetime in the river basin are in the same order of magnitude as the inputs. The

490   sensitivity analysis showed that in-stream chemistry and CO_2 emissions are weakly correlated with discharge in contrast to recent regression approaches. The dominant driver of total C export, being mainly *DIC* export, is the weathering input from groundwater. CO_2 emissions are strongly responsive to temperature variability and *POC* dynamics. The sensitivity analysis also suggests that if we want to understand CO_2 emissions from river systems, floodplains are a pivotal component to consider, as increases in CO_2 emissions originate for 45% from terrestrial vegetation litter delivery to floodplains/wetlands. This may

495   be higher for tropical floodplains, as floodplains/wetlands contribute relatively much to the total water area of river basins.

Our results show that improvement in some model formulations could result in a better match of simulations with observations. Firstly, a better description of the hydrology in low-order streams to replace the current parameterization will improve our C cycle model in headwaters. The HydroSheds dataset (Lehner and Grill, 2013) is a good candidate to improve our PCR-

500   GLOBWB model. The HydroLakes dataset (Messager et al., 2016) will improve the current data on lake and reservoir water volume. Secondly, C inputs are an important source of uncertainty in terms of their spatial distribution, organic/inorganic ratios and form (dissolved or particulate). For example, an improved estimate of terrestrial *POC* input from litterfall and its variation between headwaters to wider mainstreams is necessary to provide a more robust quantification and spatial estimate of CO_2

emissions from freshwaters. Similarly, alkalinity input from groundwater is important but uncertain and can be improved by a
505 better model for weathering and *DOC* input to aquifers and transformation to *DIC*. Finally, the modelled primary production
is limited by light and carbon. A future major challenge to be tackled in global biogeochemical modelling frameworks is to
introduce limitations to primary production imposed by nutrients (nitrogen, phosphorus and silicium) and oxygen availability.

Code and data availability

510 The presented version of CARBON-DISC is archived on Zenodo (van Hoek et al., 2019) under the Gnu Public License, GPL
v3, in the form of input data and scripts to run the model and the raw output data for all the simulations presented in this study.
Python scripts containing the source code of CARBON-DISC 1.0 are available in section A (source code). All used input data
is found in section B (model input). Raw output data for the model runs shown in the results section are found in section C
(raw output data). Data specifically to reproduce the figures are found in section D (data for figures). For further information
515 about the IMAGE-DGNM framework and the data used to produce the presented results, please contact Alexander F.
Bouwman (lex.bouwman@pbl.nl).

Author contributions

W.J. van Hoek prepared the original draft, developed the CARBON-DISC module and ran the model simulations. A.H.W.
520 Beusen and J.M. Mogollón integrated the IMAGE-GNM and PCR-GLOBWB to construct the IMAGE-DGNM framework in
which the CARBON-DISC was developed. J.J. Middelburg, A.F. Bou wman, L. Vilmin, X. Liu and J.J. Langeveld
contributed to formulate concepts and research aims.

Competing interests

525 The authors declare that they have no conflict of interest.

Acknowledgements

This work is part of The New Delta 2014 ALW project project nr 869.15.014, which is financed by the Netherlands
Organisation for Scientific Research (NWO). Alexander F. Bouwman and Arthur H. W. Beusen received support from PBL
530 Netherlands Environmental Assessment Agency through in-kind contributions to The New Delta 2014 ALW project. Lauriane
Vilmin received funding from part of the Earth and life sciences (ALW) Open Programme 2016 project no. ALWOP.230,
which is financed by the Netherlands Organisation for Scientific Research (NWO). Joep J. Langeveld received funding from
The New Delta 2014 ALW project project nr 869.15.015, which is financed by the Netherlands Organisation for Scientific
Research (NWO).

535

References

Abril, G., Bouillon, S., Darchambeau, F., Teodoru, C. R., Marwick, T. R., Tamooh, F., Ochieng Omengo, F., Geeraert, N., Deirmendjian, L., Polsenaere, P. and Borges, A. V.: Technical note: Large overestimation of pCO2 calculated from pH and alkalinity in acidic, organic-rich freshwaters, Biogeosciences, 12(1), 67–78, doi:10.5194/bg-12-67-2015, 2015.

540   Aitkenhead, J. A. and McDowell, W. H.: Soil C: N ratio as a predictor of annual riverine DOC flux at local and global scales, Global Biogeochem. Cycles, 14(1), 127–138, 2000.

Alin, S. R., Rasera, M. D. F. F. L., Salimon, C. I., Richey, J. E., Holtgrieve, G. W., Krusche, A. V. and Snidvongs, A.: Physical controls on carbon dioxide transfer velocity and flux in low-gradient river systems and implications for regional carbon budgets, J. Geophys. Res. Biogeosciences, 116(1), doi:10.1029/2010JG001398, 2011.

545   Bastviken, D., Tranvik, L. J., Downing, J. A., Crill, P. M. and Enrich-Prast, A.: Freshwater methane emissions offset the continental carbon sink, Science (80-.)., 331(6013), 50, 2011.

Batjes, N. H.: Revised soil parameter estimates for the soil types of the world, Soil Use Manag., 18(3), 232–235, doi:10.1079/SUM2002125, 2002.

Batjes, N. H.: Harmonized soil property values for broad-scale modelling (WISE30sec) with estimates of global soil carbon 550   stocks, Geoderma, 269, 61–68, 2016.

Battin, T. J., Luyssaert, S., Kaplan, L. A., Aufdenkampe, A. K., Richter, A. and Tranvik, L. J.: The boundless carbon cycle, Nat. Geosci., 2(9), 598–600, 2009.

Van Beek, L. P. H., Wada, Y. and Bierkens, M. F. P.: Global monthly water stress: 1. Water balance and water availability, Water Resour. Res., 47(7), 2011.

555   Beusen, A. H. W., Dekkers, A. L. M., Bouwman, A. F., Ludwig, W. and Harrison, J.: Estimation of global river transport of sediments and associated particulate C, N, and P, Global Biogeochem. Cycles, 19(4), 2005.

Beusen, A. H. W., Van Beek, L. P. H., Bouwman, L., Mogollón, J. M. and Middelburg, J. B. M.: Coupling global models for hydrology and nutrient loading to simulate nitrogen and phosphorus retention in surface water–description of IMAGE–GNM and analysis of performance, Geosci. Model Dev., 8(12), 4045–4067, 2015.

560   Bianchi, T. S.: The role of terrestrially derived organic carbon in the coastal ocean: A changing paradigm and the priming effect, Proc. Natl. Acad. Sci., 108(49), 19473–19481, doi:10.1073/pnas.1017982108, 2011.

Borges, A. V., Abril, G., Darchambeau, F., Teodoru, C. R., Deborde, J., Vidal, L. O., Lambert, T. and Bouillon, S.: Divergent biophysical controls of aquatic CO2 and CH4 in the World's two largest rivers, Sci. Rep., 5, 1–10, doi:10.1038/srep15614, 2015.

565   Cerdan, O., Govers, G., Le Bissonnais, Y., Van Oost, K., Poesen, J., Saby, N., Gobin, A., Vacca, A., Quinton, J., Auerswald, K., Klik, A., Kwaad, F. J. P. M., Raclot, D., Ionita, I., Rejman, J., Rousseva, S., Muxart, T., Roxo, M. J. and Dostal, T.: Rates and spatial variations of soil erosion in Europe: A study based on erosion plot data, Geomorphology, 122(1–2), 167–177, doi:10.1016/j.geomorph.2010.06.011, 2010.

Ciais, P., Sabine, C., Bala, G., Bopp, L., Brovkin, V., Canadell, J., Chhabra, A., DeFries, R., Galloway, J. and Heimann, M.:
570   Carbon and other biogeochemical cycles, in Climate Change 2013: The Physical Science Basis. Contribution of Working
Group I to the Fifth Assessment Report of the Intergovernmental Panel on Climate Change, pp. 465–570, Cambridge
University Press., 2013.

Cole, Prairie, Y. T., Caraco, N. F., McDowell, W. H., Tranvik, L. J., Striegl, R. G., Duarte, C. M., Kortelainen, P., Downing,
J. A. and Middelburg, J. J.: Plumbing the global carbon cycle: integrating inland waters into the terrestrial carbon budget,
575   Ecosystems, 10(1), 172–185, 2007.

Crawford, J. T., Striegl, R. G., Wickland, K. P., Dornblaser, M. M. and Stanley, E. H.: Emissions of carbon dioxide and
methane from a headwater stream network of interior Alaska, J. Geophys. Res. Biogeosciences, 118(2), 482–494,
doi:10.1002/jgrg.20034, 2013.

Crawford, J. T., Loken, L. C., Stanley, E. H., Stets, E. G., Dornblaser, M. M. and Striegl, R. G.: Basin scale controls on CO2
580   and CH4 emissions from the Upper Mississippi River, Geophys. Res. Lett., 1–7, doi:10.1002/2015GL067599.Received, 2016.

Duarte, C. M. and Prairie, Y. T.: Prevalence of heterotrophy and atmospheric CO2 emissions from aquatic ecosystems,
Ecosystems, 8(7), 862–870, doi:10.1007/s10021-005-0177-4, 2005.

Dürr, H. H., Meybeck, M. and Dürr, S. H.: Lithologic composition of the Earth's continental surfaces derived from a new
digital map emphasizing riverine material transfer, Global Biogeochem. Cycles, 19(4), 1–23, doi:10.1029/2005GB002515,
585   2005.

Frankignoulle, M., Abril, G., Borges, A., Bourge, I., Canon, C., Delille, B., Libert, E. and Théate, J.-M.: Carbon Dioxide
Emission from European Estuaries, Science (80-.)., 282(5388), 434–436, doi:10.1126/science.282.5388.434, 1998.

Garnier, J., Billen, G. and Palfner, L.: Understanding the oxygen budget and related ecological processes in the river Mosel:
The RIVERSTRAHLER approach, Hydrobiologia, 410, 151–166, doi:10.1023/A:1003894200796, 2000.

590   Hartmann, J., Lauerwald, R. and Moosdorf, N.: A Brief Overview of the GLObal RIver Chemistry Database, GLORICH,
Procedia Earth Planet. Sci., 10, 23–27, doi:10.1016/j.proeps.2014.08.005, 2014.

Hernes, P. J., Dyda, R. Y. and McDowell, W. H.: Connecting tropical river DOM and POM to the landscape with lignin,
Geochim. Cosmochim. Acta, 219, 143–159, doi:10.1016/j.gca.2017.09.028, 2017.

van Hoek, W. J., Vilmin, L., Beusen, A., J., M., Langeveld, J., Bouwman, A. F. and Middelburg, J. J.: Release version 1 of the
595   CARBON-Dynamic In Stream Chemistry model, , doi:10.5281/ZENODO.3402473, 2019.

Holgerson, M. A. and Raymond, P. A.: Large contribution to inland water CO2 and CH4 emissions from very small ponds,
Nat. Geosci., 9(3), 222–226, doi:10.1038/ngeo2654, 2016.

Hotchkiss, E. R., Hall Jr, R. O., Sponseller, R. A., Butman, D., Klaminder, J., Laudon, H., Rosvall, M. and Karlsson, J.: Sources
of and processes controlling CO2 emissions change with the size of streams and rivers, Nat. Geosci., 8(9), 696–699, 2015.

600   Jansen, N.: Chemical rock weathering as source of dissolved silica and sink of atmospheric CO2, Intitute Biogeochem. Mar.
Chem., Dr rer. na, 125, 2010.

Kempe, S.: Sinks of the anthropogenically enhanced carbon cycle in surface fresh waters, J. Geophys. Res., 89(D3), 4657,

doi:10.1029/JD089iD03p04657, 1984.

Kirk, J. T. O.: Light and photosynthesis in aquatic ecosystems, Third Edit., Cambridge University Press., 2011.

605 Kroeze, C., Bouwman, A. F. and Seitzinger, S. P.: Modeling global nutrient export from watersheds, Curr. Opin. Environ. Sustain., 4(2), 195–202, 2012.

Lauerwald, R., Hartmann, J., Moosdorf, N., Kempe, S. and Raymond, P. A.: What controls the spatial patterns of the riverine carbonate system? - A case study for North America, Chem. Geol., 337–338, 114–127, doi:10.1016/j.chemgeo.2012.11.011, 2013.

610 Lehner, B. and Grill, G.: Global river hydrography and network routing: Baseline data and new approaches to study the world's large river systems, Hydrol. Process., 27(15), 2171–2186, doi:10.1002/hyp.9740, 2013.

Liu, E., Yan, C., Mei, X., Zhang, Y. and Fan, T.: Long-term effect of manure and fertilizer on soil organic carbon pools in dryland farming in northwest China, PLoS One, 8(2), e56536, 2013.

Lobbes, J. M., Fitznar, H. P. and Kattner, G.: Biogeochemical characteristics of dissolved and particulate organic matter in
615 Russian rivers entering the Arctic Ocean, Geochim. Cosmochim. Acta, 64(17), 2973–2983, 2000.

Mayorga, E., Seitzinger, S. P., Harrison, J. A., Dumont, E., Beusen, A. H. W., Bouwman, A. F., Fekete, B. M., Kroeze, C. and van Drecht, G.: Global nutrient export from WaterSheds 2 (NEWS 2): model development and implementation, Environ. Model. Softw., 25(7), 837–853, 2010.

Mcdowell, W. H., Wood, T., Forest, B. E. and Thornton, W.: PODZOLIZATION : SOIL PROCESSES CONTROL
620 DISSOLVED ORGANIC CARBON CONCENTRATIONS IN STREAM WATER ' This study was conducted at the Hubbard, Soil Sci., 137(1), 23–32, 1984.

Messager, M. L., Lehner, B., Grill, G., Nedeva, I. and Schmitt, O.: Estimating the volume and age of water stored in global lakes using a geo-statistical approach, Nat. Commun., 7, 1–11, doi:10.1038/ncomms13603, 2016.

Middelburg, J. J.: A simple rate model for organic matter decomposition in marine sediments, Geochim. Cosmochim. Acta,
625 53(7), 1577–1581, doi:https://doi.org/10.1016/0016-7037(89)90239-1, 1989.

Middelburg, J. J.: Organic Matter is more than CH2O BT - Marine Carbon Biogeochemistry : A Primer for Earth System Scientists, edited by J. J. Middelburg, pp. 107–118, Springer International Publishing, Cham., 2019.

Mitchell, T. D. and Jones, P. D.: An improved method of constructing a database of monthly climate observations and associated high-resolution grids, Int. J. Climatol., 25(6), 693–712, doi:10.1002/joc.1181, 2005.

630 Moosdorf, N., Hartmann, J., Lauerwald, R., Hagedorn, B. and Kempe, S.: Atmospheric CO_2 consumption by chemical weathering in North America, Geochim. Cosmochim. Acta, 75(24), 7829–7854, doi:10.1016/j.gca.2011.10.007, 2011.

Orr, J. C. and Epitalon, J. M.: Improved routines to model the ocean carbonate system: Mocsy 2.0, Geosci. Model Dev., 8(3), 485–499, doi:10.5194/gmd-8-485-2015, 2015.

Prairie, Y. T. and Cole, J. J.: Carbon , Unifying Currency, Encycl. Inl. Waters, 2(December), 743–746,
635 doi:http://dx.doi.org/10.1016/B978-012370626-3.00107-1, 2009.

Prairie, Y. T. and Duarte, C. M.: Direct and indirect metabolic CO_2 release by humanity, Biogeosciences Discuss., 3(6), 1781–

1789, doi:10.5194/bgd-3-1781-2006, 2006.

Raymond, P. A., Hartmann, J., Lauerwald, R., Sobek, S., McDonald, C., Hoover, M., Butman, D., Striegl, R., Mayorga, E. and Humborg, C.: Global carbon dioxide emissions from inland waters, Nature, 503(7476), 355–359, 2013.

640 Regnier, P., Friedlingstein, P., Ciais, P., Mackenzie, F. T., Gruber, N., Janssens, I. A., Laruelle, G. G., Lauerwald, R., Luyssaert, S. and Andersson, A. J.: Anthropogenic perturbation of the carbon fluxes from land to ocean, Nat. Geosci., 6(8), 597–607, 2013.

Richardson, D. C., Newbold, J. D., Aufdenkampe, A. K., Taylor, P. G. and Kaplan, L. A.: Measuring heterotrophic respiration rates of suspended particulate organic carbon from stream ecosystems, Limnol. Oceanogr. Methods, 11(5), 247–261, 2013.

645 Riesebell, U., Wolf-Gladrow, D. A. and Smetacek, V.: Carbon dioxide limitation of marine phytoplankton growth rates, Nature, 361, 249–251, 1993.

Saltelli, A.: Chan. K., Scott EM (ed.), Sensitivity Analysis, 2000.

Sawakuchi, H. O., Neu, V., Ward, N. D., Barros, M. D. L. C., Valerio, A., Gagne-maynard, W., Cunha, A. C., Fernanda, D., Diniz, J. E., Brito, D. C., Krusche, A. V and Richey, J. E.: Carbon dioxide emissions along the lower Amazon River, Front.

650 Mar. Sci., 4(March), 1–12, doi:10.3389/fmars.2017.00076, 2017.

Scheffer, M.: Ecology of shallow lakes, Springer., 2004.

Sitch, S., Smith, B., Prentice, I. C., Arneth, A., Bondeau, A., Cramer, W., Kaplan, J. O., Levis, S., Lucht, W. and Sykes, M. T.: Evaluation of ecosystem dynamics, plant geography and terrestrial carbon cycling in the LPJ dynamic global vegetation model, Glob. Chang. Biol., 9(2), 161–185, 2003.

655 Soetaert, K. and Herman, P. M. J.: A practical guide to ecological modelling: using R as a simulation platform, Springer Science & Business Media., 2008.

Soetaert, K., Hofmann, A. F., Middelburg, J. J., Meysman, F. J. R. and Greenwood, J.: Reprint of "The effect of biogeochemical processes on pH," Mar. Chem., 106(1), 380–401, doi:https://doi.org/10.1016/j.marchem.2007.06.008, 2007.

Stehfest, E., van Vuuren, D., Kram, T., Bouwman, L., Alkemade, R., Bakkenes, M., Biemans, H., Bouwman, A., den Elzen,

660 M., Janse, J., Lucas, P., van Minnen, J., Muller, C. and Prins, A. G.: Integrated Assessment of Global Environmental Change with IMAGE 3.0. Model description and policy applications. [online] Available from: http://www.pbl.nl/en/publications/integrated-assessment-of-global-environmental-change-with-IMAGE-3.0, 2014.

Stelzer, R. S., Heffernan, J. and Likens, G. E.: The influence of dissolved nutrients and particulate organic matter quality on microbial respiration and biomass in a forest stream, Freshw. Biol., 48(11), 1925–1937, doi:10.1046/j.1365-

665 2427.2003.01141.x, 2003.

Strokal, M., Kroeze, C., Wang, M., Bai, Z. and Ma, L.: The MARINA model (Model to Assess River Inputs of Nutrients to seAs): Model description and results for China, Sci. Total Environ., 562, 869–888, doi:10.1016/j.scitotenv.2016.04.071, 2016.

Sutanudjaja, E. H., Beek, R. van, Wanders, N., Wada, Y., Bosmans, J. H. C., Drost, N., Ent, R. J., De Graaf, I. E. M., Hoch, J. M. and Jong, K. de: PCR-GLOBWB 2: a 5 arcmin global hydrological and water resources model, Geosci. Model Dev., 11(6),

670 2429–2453, 2018.

Tranvik, L. J., Downing, J. A., Cotner, J. B., Loiselle, S. A., Striegl, R. G., Ballatore, T. J., Dillon, P., Finlay, K., Fortino, K., Knoll, L. B., Kortelainen, P. L., Kutser, T., Larsen, S., Laurion, I., Leech, D. M., McCallister, S. L., McKnight, D. M., Melack, J. M., Overholt, E., Porter, J. A., Prairie, Y., Renwick, W. H., Roland, F., Sherman, B. S., Schindler, D. W., Sobek, S., Tremblay, A., Vanni, M. J., Verschoor, A. M., von Wachenfeldt, E. and Weyhenmeyer, G. A.: Lakes and reservoirs as

675   regulators of carbon cycling and climate, Limnol. Oceanogr., 54(6), 2298–2314, doi:10.4319/lo.2009.54.6_part_2.2298, 2009.

Uehlinger, U., Wantzen, K. M., Leuven, R. S. E. W. and Arndt, H.: The Rhine River Basin., 2009.

Vilmin, L., Mogollón, J. M., Beusen, A. H. W. and Bouwman, A. F.: Forms and subannual variability of nitrogen and phosphorus loading to global river networks over the 20th century, Glob. Planet. Change, 163(February), 67–85, doi:10.1016/j.gloplacha.2018.02.007, 2018.

680   Vilmin, L., Mogollón, J. M., Beusen, A. H. W., van Hoek, W. J., Liu, X., Middelburg, J. J. and Bouwman, A. F.: Modelling process-based biogeochemical dynamics in surface freshwaters with the {IMAGE-DGNM} framework, Environ. Model. Softw., 2019.

Wallin, M. B., Grabs, T., Buffam, I., Laudon, H., Ågren, A., Öquist, M. G. and Bishop, K.: Evasion of CO2 from streams - The dominant component of the carbon export through the aquatic conduit in a boreal landscape, Glob. Chang. Biol., 19(3),

685   785–797, doi:10.1111/gcb.12083, 2013.

Wanninkhof, R.: Relationship between wind speed and gas exchange over the ocean revisited, Limnol. Oceanogr. Methods, 12(JUN), 351–362, doi:10.4319/lom.2014.12.351, 2014.

van der Weijden, C. H. and Middelburg, J. J.: Hydrogeochemistry of the river rhine: long term a n d seasonal variability, elemental budgets, base levels a n d pollution, , 23(10), 1247–1266, 1989.

690   Wollheim, W. M., V??r??smarty, C. J., Bouwman, A. F., Green, P., Harrison, J., Linder, E., Peterson, B. J., Seitzinger, S. P. and Syvitski, J. P. M.: Global N removal by freshwater aquatic systems using a spatially distributed, within-basin approach, Global Biogeochem. Cycles, 22(2), 1–14, doi:10.1029/2007GB002963, 2008.

Wollheim, W. M., Stewart, R. J., Aiken, G. R., Butler, K. D., Morse, N. B. and Salisbury, J.: Removal of terrestrial DOC in aquatic ecosystems of a temperate river network, Geophys. Res. Lett., 42(16), 6671–6679, 2015.

695

700

705

Table 1: Sources of C to surface waters as shown in fig. 03 and description of their calculation

source	description
DOC input from waste water (*WAS$_{DOC}$*)	Global organic carbon from waste is obtained from estimates by (Prairie and Duarte, 2006) is combined with the spatio-temporal estimates of P in wastewater from Vilmin et al. (2018) to obtain *DOC* in waste water from (Vilmin et al., 2018). All organic carbon in waste water is assumed to be in dissolved form.
DOC input from surface runoff (*SRO$_{DOC}$*)	*DOC* in soil moisture is transported to the oceans via rivers ((Mcdowell et al., 1984; Aitkenhead and McDowell, 2000; Lobbes et al., 2000; Hernes et al., 2017). *DOC* in soil moisture enters surface freshwaters via surface runoff. *DOC* in soil moisture is related to the soil organic carbon (fSOC) (Liu et al., 2013). The dissolved fraction of the total soil organic carbon is here assumed to 1%. A spatial distribution of SOC is obtained from (Batjes, 2016). SOC [%] is multiplied with bulk density [kg/dm^3] ((Batjes, 2002), which gives the mass density of soil organic carbon [kg/dm^3]. Multiplication of the soil organic carbon mass density with monthly surface runoff from (Van Beek et al., 2011)
POC$_{terre}$ input from soil loss (*SOI$_{POC}$*)	Soil erosion delivers terrestrial *POC* in freshwaters parallel to an approach proposed by (Cerdan et al., 2010) based on slope, soil texture and land cover type. Country aggregated soil loss rates for arable land, grassland and natural vegetation were applied to all grid cells with each their own areal fraction of arable land, grassland and natural vegetation. The soil loss enters the surface

	waters as SPM. To account for the POC_{terre}, SPM input is multiplied with f_{SOC} from (Batjes, 2016) to obtain the *fPOC* in eroded soil.
POC_{terre} input from litterfall (LIT_{POC})	Terrestrial *POC* input from litterfall is based on IMAGE estimates of C production with NPP for wetlands and floodplains from the LPJ model (Sitch et al., 2003). In the DISC module, POC_{terre} from litterfall enters surface waters in two ways. 1: via riparian zones of small streams 50% of total NPP within the areal fraction of riparian zones (of 1 meter wide) is assumed to end in the stream 2: via floodplains along the mainstream 100% of total NPP within the floodplain area is considered to end up in the floodplain surface waters.
DIC/Alkalinity input from weathering (WEA_{DIC})	Lithology and discharge are the strongest controllers for annual bicarbonate fluxes for 338 catchments basin across North America. (Jansen, 2010; Moosdorf et al., 2011; Lauerwald et al., 2013). Here we apply the empirical parameterization for annual bicarbonate fluxes from (Jansen, 2010). We use lithological data from (Dürr et al., 2005). All the *DIC* input from this source is assumed to be bicarbonate.

710

Table 2: Parameters , units, values and literature references

parameter	unit	value	reference
$C_{atmosphere}$	mmol L^{-1}	0.0136 (400ppm)	-
a_1	-	4.46	(Alin et al., 2011)
b_1	-	7.11	(Alin et al., 2011)
a_2	-	13.82	(Alin et al., 2011)
b_2	-	0.35	(Alin et al., 2011)
k_{DOCmin}	day^{-1}	0.04	(Richardson et al., 2013)

η_{DOC}	m^{-1} mg^{-1} L	0.01	(Scheffer, 2004)
$k_{POCterre\_min}$	day^{-1}	0.01	(Richardson et al., 2013)
$Q10_{POCterre}$	-	2	(Soetaert and Herman, 2008)
$\eta_{POCterre}$	m^{-1} mg^{-1} L	0.05	(Scheffer, 2004)
$vsed_{POCterre}$	km yr^{-1}	4.38	(Vilmin et al., 2019)
$k_{SEDOCterre\_min}$	day^{-1}	0.001	(Richardson et al., 2013)
$Q10_{SEDOCterre}$	-	2	(Soetaert and Herman, 2008)
$k_{POCauto\_min}$	day^{-1}	0.02	(Richardson et al., 2013)
$Q10_{POCauto}$	-	2	(Soetaert and Herman, 2008)
$\eta_{POCauto}$	m^{-1} mg^{-1} L	0.03	(Scheffer, 2004)
$vsed_{POCauto}$	km yr^{-1}	4.38	(Vilmin et al., 2019)
$k_{SEDOCauto\_min}$	day^{-1}	0.02	(Richardson et al., 2013)
$Q10_{SEDOCauto}$	-	2	(Soetaert and Herman, 2008)
k_{burial}	day^{-1}	0.024	-
k_{ALG_pp}	day^{-1}	4.8	(Garnier et al., 2000)
k_{I_ALG}	W m^{-2}	25	(Garnier et al., 2000)
k_{DIC_ALG}	mmol L^{-1}	0.001	(Riesebell et al., 1993)
k_{ALG_resp}	day^{-1}	0.072	(Garnier et al., 2000)
k_{ALG_mort}	day^{-1}	0.096	(Garnier et al., 2000)
k_{ALG_excr}	day^{-1}	0.072	(Garnier et al., 2000)
vf_{ALG} *(parasitic lysis amplification)*	-	20	(Garnier et al., 2000)
$p\_threshold_{ALG}$	mmol C L^{-1}	0.019	(Garnier et al., 2000)
$k_{ALG\_benth\_pp}$	day^{-1}	1.5	(Garnier et al., 2000)
$k_{I\_ALG\_benth}$	W m^{-2}	12.5	(Garnier et al., 2000)
$k_{DIC\_ALG\_benth}$	mmol L^{-1}	0.001	(Riesebell et al., 1993)
$k_{ALG\_benth\_resp}$	day^{-1}	0.072	(Garnier et al., 2000)
$k_{ALG\_benth\_mort}$	day^{-1}	0.096	(Garnier et al., 2000)

$k_{ALG\_benth\_excr}$	day^{-1}	0.072	(Garnier et al., 2000)
vf_{ALG_benth}	-	20	(Garnier et al., 2000)
(parasitic lysis amplification)			
$p\_threshold_{ALG\_benth}$	mmol C L^{-1}	0.019	(Garnier et al., 2000)

715

Table 3: Model parameters and units

parameter	meaning
WAS_{DOC}	dissolved organic carbon in waste water [Mmol yr^{-1}]
$LIT_{POCterre}$	particulate organic carbon in litterfall [Mmol yr^{-1}]
WEA_{DIC}	dissolved organic carbon in weathering [Mmol yr^{-1}]
$SOI_{POCterre}$	particulate organic carbon in soil loss [Mmol yr^{-1}]
LEA_{DOC}	dissolved organic carbon in soil leaching water [Mmol yr^{-1}]
WAS_{DOC}	dissolved organic carbon in waste water [Mmol yr^{-1}]
$fDOC$	mass fraction of dissolved organic carbon [-]
$fSOC$	mass fraction of soil organic carbon [-]
ρ_b	soil dry bulk density [kg dm^{-3}]
soil$_{ro}$	soil runoff [mm yr^{-1}]
TSS	total suspended solids [Mmol]
NPP	net primary production [Mmol yr^{-1}]
$f_{wetlands}$	areal fraction of wetlands [-]
$f_{floodplains}$	areal fraction of floodplains [-]
b_0	empirical parameter used to calculate alkalinity discharge
A_L	area with lithological class L [km^2]
Q	discharge [km^3 yr^{-1}]
b_L	empirical parameter accounting for effect of lithological class L on alkalinity discharge
v	flow velocity in order I [cm s^{-1}]

A_b	stream bed area [km^2]
D	stream depth [m]
w	stream width [m]
u_{10}	windspeed at 10 meters above water surface [m s^{-1}]
F_{high_veg}	high vegetation fraction
F_{u10_veg}	wind speed reduction under high vegetation
k600	Gas exchange rate at 20°C [cm h^{-1}]
Sc_T	Schmidt number for temperature T
η	parameter to represent the effect of a biogeochemical specie on light extinction in the water column
T	water temperature [°C]
I_0	solar radiation at water surface [W m^{-2}]
I_z	light at depth z in the water column [W m^{-2}]
k_I	half saturation for light limitation with Michaelis-Menten [W m^{-2}]
k_DIC	half saturation for DIC limitation with Michaelis-Menten [mmol L^{-1}]

Table 4: SRC values of most relevant parameters and results obtained from the sensitivity analysis. In green the most important
720 **positive SRC's, in red the most important negative SRC's.**

			CO₂ exchange				TC	POC
parameter	total	headwaters	main stream	lakes	reservoirs	floodplains	export	retention
Q	-0.01	-0.06	-0.11	-0.18	-0.11	0.06	0.34	-0.06
T	0.27		0.04	0.11	0.08	0.32	-0.07	-0.50
I_0	-0.24		-0.08	-0.04	-0.07	-0.28	0.10	0.03
$k_{SEDOCterre\_min}$	0.28		0.03	0.04	0.05	0.34	-0.02	-0.36
k_{sedbur}	-0.22		-0.02	-0.03	-0.05	-0.28	0.02	0.23
k_{sedlim}	0.16		0.01	0.01	0.02	0.21	-0.02	-0.15
WEA_{DIC}	0.43	0.72	0.71	0.69	0.69	0.07	0.01	
WEA_{ALK}	-0.42	-0.70	-0.68	-0.67	-0.67	-0.07	0.90	
$LIT_{POC\_floodplains}$	0.45		0.03	0.02		0.57	0.09	0.55